



A parameter extraction technique exploiting intrinsic properties of solar cells



Nhan Thanh Tong, Wanchalerm Pora^{*}

Department of Electrical Engineering, Chulalongkorn University, Bangkok, Thailand

HIGHLIGHTS

- With two intrinsic properties, a simple parameter extraction is proposed.
- The proposed method requires less measured points than the existing ones.
- Mean Absolute Error is lower than that of the existing methods.

ARTICLE INFO

Article history:

Received 26 December 2015
Received in revised form 12 April 2016
Accepted 9 May 2016
Available online 14 May 2016

Keywords:

Solar cell
Parameter extraction
Maximum power point

ABSTRACT

This paper presents a parameter extraction technique for the five-parameter solar-cell model. It only requires the priori knowledge of three load points: the open circuit, the short circuit, and the maximum power points. An intrinsic property of solar cells helps to construct an extra equation. A cost function is formulated with another intrinsic property. A search algorithm for minimizing the cost function is proposed. The best set of parameters is revealed at the end of searching. Two load scanning experiments are performed on two different solar panels. The simulated I – V curves, produced with the obtained parameters, match the empirical measured results nicely. When compared to other existing techniques, our proposed method usually yields less mean absolute error.

© 2016 The Authors. Published by Elsevier Ltd. This is an open access article under the CC BY-NC-ND license (<http://creativecommons.org/licenses/by-nc-nd/4.0/>).

1. Introduction

Over the last few decades, the world has witnessed a significant increase in the installed capacity of photovoltaic (PV) systems. Because every PV system is composed principally of solar cells. Knowing parameters of solar cells at various operating conditions is of great importance, as it helps to produce the I – V curve of the PV system. Then its maximum power point may be estimated. Manufacturers of solar cells or PV panels usually publish the curves at only a few operating conditions. Some publish only the I – V pairs at a few load points. Fortunately, a solar cell can be represented by a model, which is composed of a few electrical components [1]. Parameters for the model may be extracted from that limited information. Then the I – V relation at other operating conditions and/or operating loads can be estimated.

There have been a large number of studies on solar cell models (and parameter extraction) in recent years [2–4], but only a few models are widely accepted. The single-diode model (see Fig. 1)

is the most favorite one, because its relevant equations are simpler, and for most commercial PV panels, it is almost as accurate as the double diode (two diodes in parallel) or the triple model (three diodes in parallel). It only has five parameters: (1) the induced current (or photo generated current) I_{ph} , (2) the saturation current (or dark current) I_s , (3) the emission coefficient (or ideality factor) n , (4) the series resistance R_s , and (5) the shunt (or parallel) resistance R_p .

Almost all parameter extraction methods rely on the well-known I – V equation of solar cells. Based on their complexity, these studies can be categorized into two groups. Methods in the first group usually estimate value of one or two parameters and require just a few measurements. So they are quite simple, but their extraction results are not accurate. Methods in the second group require a lot of measurements and complex calculation, so they yield good extraction.

For the first group, all methods exploit the fact that some parameters can be estimated with good accuracy when the solar cells are forced to operate at the short-circuited point (SCP) and/or the open-circuited point (OCP). A parameter extraction method called “Five Points” [5], uses two approximations: $R_p \approx -\frac{dV}{dI}|_{I=I_{SC}}$ and $R_s \approx -\frac{dV}{dI}|_{V=V_{OC}}$, where I_{SC} and V_{OC} denote the current when the cells

^{*} Corresponding author.

E-mail addresses: tongthanhnhan@gmail.com (N.T. Tong), wanchalerm.p@chula.ac.th (W. Pora).

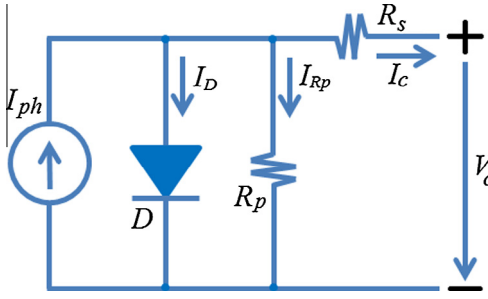


Fig. 1. An equivalent circuit of a solar cell, which is composed of a diode.

are short-circuited, and the voltage when they are open-circuited (no load) respectively. These parameters are employed to construct the I – V equations at three points: OCP, SCP, and the maximum power point (MPP). For convenience, these three special points will be later called OSMP. Solving these three equations reveals the values of three remaining parameters: I_s , I_{ph} , and n . Another method [6] also approximates R_p in the same way as [5], and it employs the fact that $e^{\frac{V_{OC}-I_{SC}R_s}{nV_T}} \approx 0$ to formulate an expression of δ as a function of n and R_s . Then n and R_s are scanned to find the most suitable set of parameters. The I – V curve computed from each parameter set is compared against the I – V curve constructed from numerous measurements of I – V points. The set that yields minimum mean squared error is the end result. The method in [7] uses only one approximation: $I_{ph} \approx I_{SC}$. Measured values at four load points are employed to calculate a and b . Both are then combined with I_{SC} and V_{OC} in order to determine the values of n , R_s , R_p and I_s . In [8] R_p is estimated by two measured points near the SCP. The “curve fitting” method is also utilized there. The other parameters are obtained by fitting at least three more load points to a curve of a special function. The extraction method in [9] uses the fact that $I_{ph} \approx I_{SC}$ and assumes that $I_{SC} \gg I_s$ to determine the values of all five parameters. The “Analytical and quasi-explicit four arbitrary point” method in [10] is a recent technique, which can be used to extract five parameters, but requires fewer measured load points.

Methods in the second group yield the parameters based on several measured points without any approximation. In [11], “polynomial curve fitting technique and Lambert W function” are employed. In [12], a modified Newton–Raphson method (with the Levenberg parameter) is employed together with the non-linear least squares optimization algorithm. The measured values presented in [12], are later used as standard datasets by many papers. With the datasets, computation techniques such as least squares [13,14], Differential Evolution (DE) [15], a modification of DE technique (P-DE) [16], Genetic Algorithm (GA) [17], Pattern Search (PS) [18], Teaching–Learning [19], Bird Mating Optimizer (BMO) [20], Chaos Particle Swarm Algorithm (CPSO) [21], Artificial Bee Swarm Optimization (ABSO) [22], and Simulated Annealing algorithm (SA) [23], are employed to find the most suitable parameters. The “mutative-scale parallel chaos optimization algorithm” (MPCOA) with crossover and merging operation is presented in [24]. Another method, which combines Levenberg Marquardt algorithm with simulated annealing, is presented in [25].

We proposed a parameters extraction technique that does not require a lot of measurements nor complex computation. In other words, it belongs to the first group, but it yields highly accurate results. This can be observed by lower mean absolute of error (MAE) when compared to a few methods in the second group. Exploiting two intrinsic properties of solar cells, it requires only measured voltages and/or currents at the OSMP. This requirement is less than or equal to that of existing methods.

Next section reviews the mathematical expressions of a conventional solar cell and PV panel. Section 3 recalls three I – V equations, when solar cells operate at the OSMP. The fourth equation is derived from an intrinsic property at the MPP. Exploiting another property, a cost function is also derived. Moreover, a searching algorithm is proposed in order to minimize the cost. In Section 4, the parameters obtained by the technique in previous section are used to produce the I – V curves, and then the results are compared with the outcomes of other existing methods. The extraction results of some commercial solar panels at STC and/or NOCT are also shown to confirm the usefulness of proposed technique.

2. Mathematical models

A solar cell can be equivalently modeled by a circuit of few discrete electrical components. PV panels are basically solar cells connected in series, so their mathematical model can easily be derived from that of solar cells.

2.1. Solar cells

Almost all conventional solar cells can be viewed as large-area p – n junctions that are subject to being hit by photons. A cell produces the photo-generated current I_{ph} , in respect of the photon flux or irradiance I_r . Hence, an ideal solar cell can be seen as a current source in parallel with a diode. The diode D includes two parameters: the ideality factor n and the saturation current I_s . In practice, a solar cell is built such that it contains parasitic components, which can be modeled as a shunt or parallel resistor R_p and a series resistor R_s . The equivalent circuit of a realistic PV cell is depicted in Fig. 1. The cell output current I_c is equal to I_{ph} minus I_D and I_{Rp} , which are the current flowing through D , and through R_p respectively. Relation between I_c and the cell terminal voltage V_c is given by

$$I_c = I_{ph} - I_s \left(e^{\frac{V_c + I_c R_s}{nV_T}} - 1 \right) - \frac{V_c + I_c R_s}{R_p} \quad (1)$$

where $V_T = \frac{kT}{q}$ is the thermal voltage, which depends on the junction temperature T , the Boltzmann's constant k , and the elementary charge constant q .

2.2. PV panels

A panel is conventionally composed of C cells connected in series (Fig. 2). Hence, the current of the panel I is always equal to I_c . Assuming that all the cells are identical and they receive the same level of photon flux, so they produce the same current and voltage.

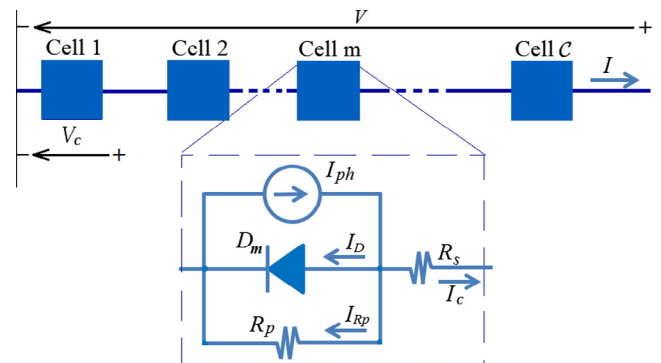


Fig. 2. Typical electrical structure of solar panels.

The terminal voltage of a solar panel V is obviously equal to CV_c . The I – V relation of the panel can be written as

$$I_{ph} - I_S(e^{\frac{V+CI R_s}{nCV_T}} - 1) - \frac{V+CI R_s}{CR_p} - I = 0 \quad (2)$$

or

$$V = nCV_T \ln \left(\frac{CI_{ps}R_p - CIR_{ps} - V}{CR_p I_S} \right) - CIR_s \quad (3)$$

where $I_{ps} = I_{ph} + I_S$ and $R_{ps} = R_p + R_s$.

3. The proposed technique

Following most existing methods, we also employ the I – V relation to gain three equations from priori knowledge of the OSMP. By combining an intrinsic property of the solar cells at the MPP with the I – V relation evaluated at the SCP, the fourth equation is formulated without further knowledge. Though the MPP condition has been used in many papers, but this combination is, to the best of authors' knowledge, new. A cost function, which is formulated with an approximation, is proposed. The approximation exploits another intrinsic property of solar cells. A search algorithm, which utilizes the five relations, is also suggested.

3.1. Three equations obtained from the priori knowledge

Substitute values of V_{OC} , I_{SC} , and the pair of voltage and current at the MPP into (2), the well-known three equations are obtained. At the OCP ($V = V_{OC}$ and $I = 0$), (2) becomes

$$I_{ph} - I_S(e^{\frac{V_{OC}}{nCV_T}} - 1) - \frac{V_{OC}}{CR_p} = 0 \quad (4)$$

At the SCP ($V = 0$ and $I = I_{SC}$), (2) becomes

$$I_{ph} - I_S(e^{\frac{I_{SC}R_s}{nCV_T}} - 1) - \frac{I_{SC}R_{ps}}{R_p} = 0 \quad (5)$$

And when the panels operate at the MPP, we get

$$I_{ph} - I_S(e^{\frac{V_M+CI_M R_s}{nCV_T}} - 1) - \frac{V_M+CI_M R_s}{CR_p} - I_M = 0 \quad (6)$$

where V_M and I_M denote the terminal voltage and the output current of the panels operating at the MPP respectively.

3.2. Fourth equation from an intrinsic property at MPP

Derivative of (2) with respect to V can be expressed as

$$-\frac{dI}{dV} = \frac{1 + \frac{dI}{dV} CR_s}{nCV_T} I_S e^{\frac{V+CI R_s}{nCV_T}} + \frac{1 + \frac{dI}{dV} CR_s}{CR_p} \quad (7)$$

It is well-known that at MPP, $\frac{dP}{dV} = 0$, and that leads to

$$\left. \frac{dI}{dV} \right|_{MPP} = -\frac{I_M}{V_M} \quad (8)$$

Using relation in (8), the derivative at MPP in (7) helps to find I_S as

$$I_S = \frac{nV_T(CI_M R_p - \beta)}{\beta R_p e^{\frac{V_M+CI_M R_s}{nCV_T}}} \quad (9)$$

where $\alpha = V_M + CI_M R_s$ and $\beta = V_M - CI_M R_s$.

3.3. Cost function from another intrinsic property

Rearrange (5) so that

$$I_{SC} R_{ps} = R_p I_{ps} (1 - \psi) \quad (10)$$

where $\psi = \frac{I_S}{I_{ps}} e^{\frac{I_{SC} R_s}{nCV_T}}$. It is an intrinsic property of most solar cells that the value of $\psi \cong 0$ (see the value of ψ extracted from more than 100 panels at [26]). Thus (10) may be reduced to

$$\frac{R_p}{R_{ps}} I_{ps} \cong I_{SC} \quad (11)$$

Note that (11) is the only estimation that we use. Derivative on (3) with respect to I is

$$\frac{dV}{dI} = \frac{(I R_s - nV_T) R_{ps} - R_p R_s I_{ps} + V R_s / C}{(I_{ps} R_p - I R_{ps} + nV_T) / C - V / C^2} \quad (12)$$

At the SCP, (12) becomes

$$\left. \frac{dV}{dI} \right|_{SCP} = C \frac{(I_{SC} R_s - nV_T) R_{ps} - R_p R_s I_{ps}}{(I_{ps} R_p - I_{SC} R_{ps} + nV_T)} \quad (13)$$

Apply (11) into (13) to get

$$\left. \frac{dV}{dI} \right|_{SCP} \cong C R_{ps} \quad (14)$$

Finally, the cost function ε is the difference between the LHS of (14) and that of (13) over C . It can be written as

$$\varepsilon = \frac{(I_{SC} R_s - nV_T) R_{ps} - R_p R_s I_{ps}}{I_{ps} R_p - I_{SC} R_{ps} + nV_T} - R_{ps} \cong 0 \quad (15)$$

3.4. Parameter reduction

Before solving Eqs. (4)–(6), (9) and relation in (15) that contains five variables, it is possible to manipulate them in order to get rid of some variables so that the solution can be found easily. Because n and R_s are on the exponents, which are difficult to be eliminated, therefore only I_{ph} , I_S , and R_p will be removed. First, subtract (5) with (4) to eliminate I_{ph} . Then I_S can be written as

$$I_S = \frac{I_{SC} C (R_p + R_s) - V_{OC}}{C R_p (e^{\frac{V_{OC}}{nCV_T}} - e^{\frac{I_{SC} R_s}{nCV_T}})} \quad (16)$$

Similarly the difference between (6) and (4) yields

$$I_S = \frac{I_M C (R_p + R_s) - V_{OC} + V_M}{C R_p (e^{\frac{V_{OC}}{nCV_T}} - e^{\frac{V_M+CI_M R_s}{nCV_T}})} \quad (17)$$

The difference between (9) and (16) eliminates I_S . Then R_p can be written in term of a function of n and R_s as

$$R_p = \frac{\beta(nCV_T(A - B) + CI_{SC} R_s - V_{OC})}{C^2 nV_T I_M (A - B) - CI_{SC} \beta} \quad (18)$$

where $A = e^{\frac{V_{OC}-\alpha}{nCV_T}}$ and $B = e^{\frac{CI_{SC} R_s - \alpha}{nCV_T}}$. In the same way, difference between (9) and (17) leads to another expression of R_p as

$$R_p = \frac{\beta(nCV_T(A - 1) - V_{OC} + \alpha)}{C^2 nV_T I_M (A - 1) - CI_M \beta} \quad (19)$$

With (18) and (19), R_p can obviously be eliminated and that leads to

$$\begin{aligned} nCV_T(I_{SC} V_M(A - 1) - I_M V_{OC}(B - 1) - 2I_M V_M(A - B)) + I_{SC} V_M^2 \\ + CI_M(I_{SC}(V_{OC} - V_M) - I_M V_{OC})R_s - V_{OC} V_M(I_{SC} - I_M) \\ = 0 \end{aligned} \quad (20)$$

which is an equation of two unknowns: R_s and n .

3.5. The search algorithm

This paper proposes a simple algorithm, which is a loop of search process. Each loop is mainly composed of three steps and

a procedure to find n for the next loop as shown in Fig. 3. The search starts with $n = 1.0$. It ends when the ten-thousandth digit of n is found. For commercial solar cells, it is well-known that $n \in [1, 2]$ and $R_s < 5 \Omega \text{ cm}^2$ [27].

3.5.1. Step 1: Search R_s from given n

When a fixed value is given to n , R_s becomes the sole variable in (20). Let the LHS of (20) is $F(R_s)$. Solving $F(R_s) = 0$ analytically is almost impossible due to its complex form. The well-known Newton–Raphson (N–R) iterative method is proposed to search for its solution.

The derivative of $F(R_s)$ with respect to R_s is

$$F'(R_s) = 2C I_M^2 V_M (A - B) - C I_M (I_{SC} V_M A - I_M V_{OC} B) + C I_M I_{SC} (V_{OC} - V_M) - C I_M^2 V_{OC}$$

The solution is determined by the following iterative formula:

$$R_s^{(i+1)} = R_s^{(i)} - \frac{F(R_s^{(i)})}{F'(R_s^{(i)})} \quad (21)$$

The iterative calculation begins with the initial $R_s^{(0)} = 1 \text{ m}\Omega$ and stops when $|R_s^{(i)} - R_s^{(i+1)}| < 0.01 \text{ m}\Omega$. With this initial value, we find empirically that (21) always converges after less than five loops.

3.5.2. Step 2: Evaluate R_p , I_s and I_{ph}

With given n and solved R_s , the other parameters, which include R_p , I_s and I_{ph} , can be evaluated using (18), (9), and (4) respectively. However, to reduce calculation error that may propagate from R_s to R_p , to I_s and finally to I_{ph} , it is safer to formulate I_s and I_{ph} in term of n and R_s only. Note that R_p in (18) or (19) is already the function of only n and R_s . Similar to Section 3.4, manipulations on three equations, including (4)–(6), may eliminate two variables. After some substitutions, I_s can be evaluated from only n and R_s by

$$I_s = \frac{((I_{SC} - I_M)V_{OC} - I_{SC}V_M)e^{-\frac{\alpha}{nqV_T}}}{\alpha(B - A) + C I_{SC} R_s (A - 1) - V_{OC}(B - 1)} \quad (22)$$

and I_{ph} may be calculated from only n and R_s by

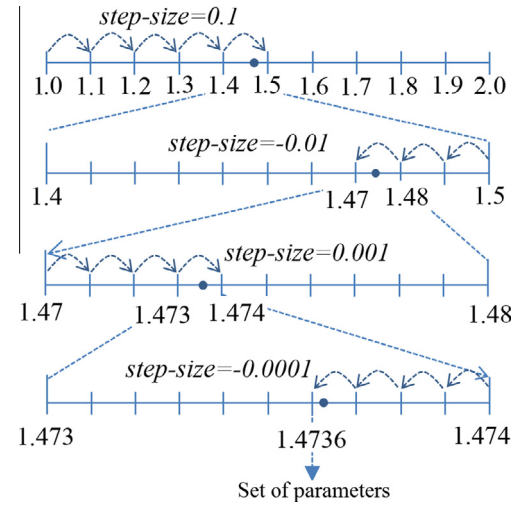


Fig. 4. An example of scanning for the most suitable value of n . When the direction changes the $step_size$ reduces ten times.

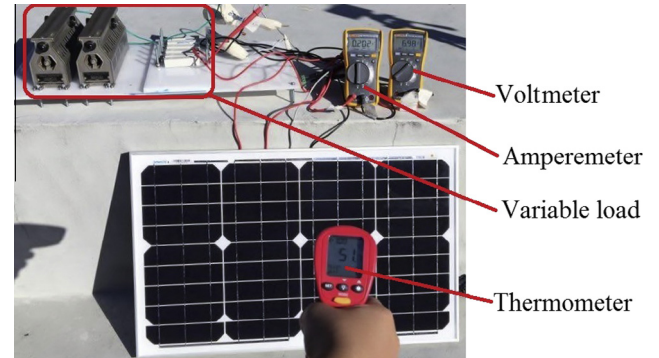


Fig. 5. Experiment for acquiring an I – V dataset from a PV panel.

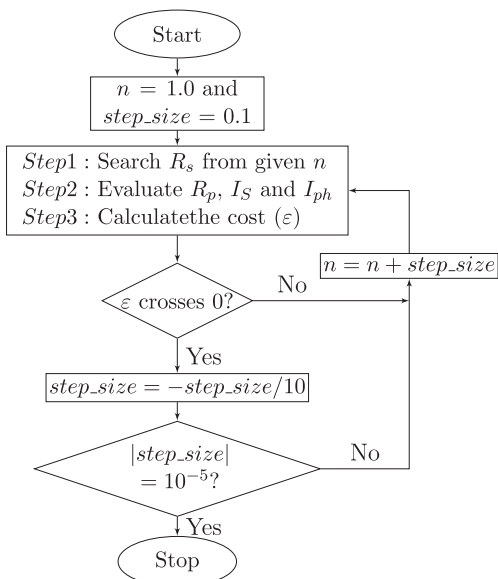


Fig. 3. Searching algorithm of the proposed method.

Table 1

Measured I – V pairs and the absolute difference between the measured and the calculated current. The experiment is performed on polycrystalline, model STP6 – 120/36 by Schutten Solar.

| | Measured | | Calculated | |
|---------|----------|-------|------------|------------|
| | V (V) | I (A) | I (A) | Error (%) |
| 1 | 17.65 | 3.83 | 3.8360 | 0.157 |
| 2 | 17.41 | 4.29 | 4.2800 | 0.233 |
| 3 | 17.25 | 4.56 | 4.5541 | 0.042 |
| 4 | 17.10 | 4.79 | 4.7940 | 0.063 |
| 5 | 16.90 | 5.07 | 5.0930 | 0.454 |
| 6 | 16.76 | 5.27 | 5.2870 | 0.323 |
| 7 | 16.34 | 5.75 | 5.7940 | 0.765 |
| 8 | 16.08 | 6.00 | 6.0550 | 0.917 |
| 9 | 15.71 | 6.36 | 6.3691 | 0.143 |
| 10 | 15.39 | 6.58 | 6.5881 | 0.123 |
| 11 | 14.93 | 6.83 | 6.8334 | 0.050 |
| 12 | 14.58 | 6.97 | 6.9748 | 0.069 |
| 13 | 14.17 | 7.10 | 7.1014 | 0.020 |
| 14 | 13.59 | 7.23 | 7.2265 | 0.048 |
| 15 | 13.16 | 7.29 | 7.2898 | 0.003 |
| 16 | 12.74 | 7.34 | 7.3345 | 0.075 |
| 17 | 12.36 | 7.37 | 7.3643 | 0.077 |
| 18 | 11.81 | 7.38 | 7.3947 | 0.199 |
| 19 | 11.17 | 7.41 | 7.4174 | 0.100 |
| 20 | 10.32 | 7.44 | 7.4352 | 0.065 |
| 21 | 9.740 | 7.42 | 7.4426 | 0.305 |
| 22 | 9.060 | 7.45 | 7.4487 | 0.017 |
| MAE (%) | | | | 0.193 |

$$I_{ph} = \frac{V_{OC}(EI_{SC} - DI_M)}{E(V_{OC} - CI_{SC}R_s) - D(V_{OC} - \alpha)} \quad (23)$$

where :

$$D = CI_{SC}R_s(e^{\frac{V_{OC}}{nV_T}} - 1) - V_{OC}(e^{\frac{I_{SC}R_s}{nV_T}} - 1)$$

$$E = \alpha(e^{\frac{V_{OC}}{nV_T}} - 1) - V_{OC}(e^{\frac{\alpha}{nV_T}} - 1)$$

3.5.3. Step 3: Calculate the cost

When a value of n is given, R_s , R_p , I_s , and I_{ph} can always be determined as shown in Step 1 and Step 2. At this point, the task is to determine which set of parameters are the most suitable for the solar cell. In this step, the cost ε is evaluated using (15) with parameters obtained from Step 1 and Step 2. The set of parameters that yields the lowest cost should be the answer.

3.5.4. Scanning strategy

Fig. 3 also shows the scanning strategy for finding the parameters that minimize the cost function. First n is 1.0 (the lowest plausible value) and the *step_size* is +0.1, complete the three steps mentioned above. Check if ε crosses zero (or changes its sign) when compared to its previous value. If not, change the value of n with the same *step_size*. But if ε crosses zero, which means the true n is between the current n and the previous one, change the direction of scanning and reduce the *step_size* ten times before moving to the next n . Continue the scanning until the *step_size* is considerably insignificant (10^{-5}). Fig. 4 shows a scanning example. First, n is scanned up from 1 with the *step_size* of +0.1. When $n = 1.5$, ε changes its sign. Then, the value of n reduced from 1.5 with *step_size* -0.01 until $n = 1.47$, ε changes its sign again. At this points the *step_size* = +0.001 so n increases again until $n = 1.474$. Then it is reduced with the *step_size* of -0.0001. Finally when $n = 1.4736$, the scanning stops. The current set of parameters found in Step 1 and Step 2 is the answer.

4. Experiment and calculation results

To verify the correctness of the proposed method, two load scanning are performed on two different PV panels in Section 4.1. The I - V curves, produced with the extracted parameters, are compared with the load scanning results. As mentioned earlier, two standard datasets have been used by many papers. We use these datasets too. The results of our proposed technique are compared with papers referenced in Section 4.2. We employ information from four product datasheets. We compare our results with [28], who uses the same datasheets. To confirm that the proposed technique is valid for a wide range of solar panels, the extractions are performed using the OSMP information from numerous data-sheets. Their results are shown in Appendix A. The last part presents effect of each and all parameter errors on the I - V curves.

4.1. Load scanning on two solar panels

A simple load scanning experiment has been set up to measure I - V datasets from each of two panels. Fig. 5 depicts the measurements, while a monocrystalline panel is supplying a variable load. An ampere-meter, a voltage-meter, a thermometer together with panel and variable load are all requirements for the experiment. By using a set of measured values T , V_{OC} , I_{SC} , and the I - V pair that yields highest output power $P = IV$, the proposed algorithm is able to extract the parameters. These parameters are used to create the mathematical models for the solar cell. When a value of V is given, the corresponding I can be calculated from the model. The results from calculation and from the experiment are compared in order to verify the correctness of the proposed methods.

4.1.1. Extracting for a polycrystalline panel

A commercial solar panel model STP6 – 120/36 manufactured by Schutten Solar is chosen to evaluate the proposed method in practice. This panel contains 36 polycrystalline cells aligned in series. Dimension of each cell is 156 mm × 156 mm. The experiment reveals that $V_{OC} = 19.21$ V, $I_{SC} = 7.48$ A, $V_M = 14.93$ V, $I_M = 6.83$ A, and $T = 55$ °C. Other measured I - V pairs are shown in Table 1 (left).

After calculation, the extracted parameters are as follows: $n = 1.2072$, $R_s = 4.9$ mΩ, $R_p = 9.745$ Ω, $I_s = 1.2$ μA, and $I_{ph} = 7.4838$ A. These parameters are applied into the MATLAB – Simulink's solar cell model to draw the I - V curve. The

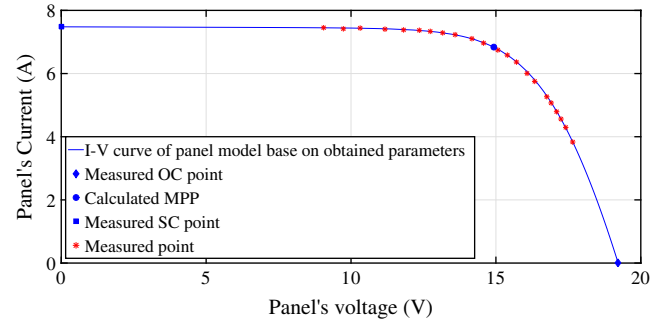


Fig. 6. I - V curve of the polycrystalline panel, modeled by the proposed method.

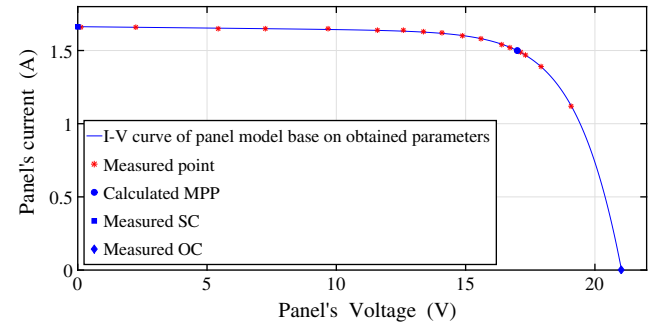


Fig. 7. I - V curve of the monocrystalline panel, modeled by the proposed method.

Table 2

Measured I - V pairs and the absolute difference between the measured and the calculated current (Model STM6 – 40/36 by Schutten Solar.)

| | Measured | | Calculated | |
|---------|----------|-------|------------|------------|
| | V (V) | I (A) | I (A) | Error (%) |
| 1 | 0.118 | 1.663 | 1.6627 | 0.012 |
| 2 | 2.237 | 1.661 | 1.6590 | 0.120 |
| 3 | 5.434 | 1.653 | 1.6531 | 0.006 |
| 4 | 7.260 | 1.650 | 1.6497 | 0.018 |
| 5 | 9.680 | 1.645 | 1.6445 | 0.030 |
| 6 | 11.59 | 1.640 | 1.6383 | 0.104 |
| 7 | 12.60 | 1.636 | 1.6330 | 0.183 |
| 8 | 13.37 | 1.629 | 1.6267 | 0.141 |
| 9 | 14.09 | 1.619 | 1.6171 | 0.117 |
| 10 | 14.88 | 1.597 | 1.6030 | 0.376 |
| 11 | 15.59 | 1.581 | 1.5820 | 0.063 |
| 12 | 16.40 | 1.542 | 1.5432 | 0.078 |
| 13 | 16.71 | 1.524 | 1.5225 | 0.098 |
| 14 | 16.98 | 1.500 | 1.5006 | 0.040 |
| 15 | 17.13 | 1.485 | 1.4867 | 0.114 |
| 16 | 17.32 | 1.465 | 1.4674 | 0.164 |
| 17 | 17.91 | 1.388 | 1.3897 | 0.122 |
| 18 | 19.08 | 1.118 | 1.1208 | 0.250 |
| MAE (%) | | | | 0.113 |

Table 3

The calculated cell parameters by the proposed method and by the other reference methods. The values in parenthesis are the difference when the values obtained by the proposed methods are compared with those of other reference methods.

| | Proposed | LMSA | CPSO | SA | PS | BMO | ABSO | GA | Newton |
|---------------------|-----------------|--------------------|--------------------|--------------------|--------------------|---------------------|--------------------|--------------------|--------------------|
| n | 1.4935 (n/a) | 1.4798 (−0.93%) | 1.5033 (0.65%) | 1.5172 (1.56%) | 1.6000 (6.66%) | 1.4817 (−0.79%) | 1.4758 (−1.20%) | 1.5751 (5.18%) | 1.4837 (−0.66%) |
| R_s (m Ω) | 36.60 (n/a) | 36.43 (−0.56%) | 35.40 (−3.49%) | 34.50 (−6.19%) | 31.30 (−17.04%) | 36.36 (−0.75%) | 36.60 (−0.09%) | 29.90 (−22.52%) | 36.40 (−0.64%) |
| R_p (Ω) | 62.574 (n/a) | 53.326 (−17.3%) | 59.012 (−6.0%) | 43.103 (−45.2%) | 64.103 (2.4%) | 53.872 (−16.2%) | 52.290 (−19.7%) | 42.373 (−47.7%) | 53.763 (−16.4%) |
| I_s (μ A) | 0.3635 (n/a) | 0.3185 (−14.1%) | 0.4000 (9.1%) | 0.4798 (24.2%) | 0.9980 (63.6%) | 0.3248 (−11.9%) | 0.3062 (−18.7%) | 0.8087 (55.0%) | 0.3223 (−12.8%) |
| I_{ph} (A) | 0.7610 (n/a) | 0.7608 (−0.03%) | 0.7607 (−0.04%) | 0.762 (+0.13%) | 0.7617 (+0.09%) | 0.76077 (−0.03%) | 0.7608 (−0.03%) | 0.7619 (+0.12%) | 0.7608 (−0.03%) |

simulated I – V curve of the proposed model together with measured points are plotted in Fig. 6. It can be seen that the curve crosses nearly all the measured points.

Table 1 (right) shows the calculated currents when the measured voltages are given, and difference between measured and calculated currents at the same voltage. The Mean Absolute Error

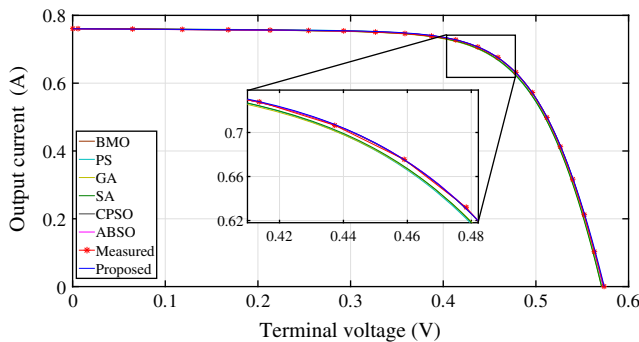


Fig. 8. I – V curves of a cell modeled by the proposed and three other reference methods.

(MAE) is only 0.193%. At all measured voltages, the differences are smaller than 1%. The discrepancy at the measured MPP is only 0.050%.

4.1.2. Monocrystalline panel

A solar panel model STM6 – 40/36 manufactured by Schutten Solar, is chosen as a representative of monocrystalline panels. The panel is composed of 36 cells in series. Size of each cell is 38 mm \times 128 mm. From the measurement: $V_{oc} = 21.02$ V, $I_{sc} = 1.663$ A, $V_M = 16.98$ V, $I_M = 1.50$ A, and temperature is 51 °C. Other measured I – V pairs are shown in Table 2 (left).

After calculation, the extracted parameters are listed as follows: $n = 1.4986$, $R_s = 4.879$ m Ω , $R_p = 15.419$ Ω , $I_s = 1.4142$ μ A, and $I_{ph} = 1.6635$ A. Again, the extracted parameters are applied into the Simulink's solar cell model to obtain the I – V curve. It is plotted together with the measured points in Fig. 7, which shows that the curve match nicely with all measured points.

Table 2 (right) displays the calculated current when V is given and absolute error at 18 measured voltages. At the MPP, discrepancy between the measured and calculated is only 0.040%. The maximum of the absolute error is 0.376% and the MAE is 0.113%.

Very low discrepancy between the measured and calculated values which are displayed in Tables 1 and 2 suggests that both

Table 4

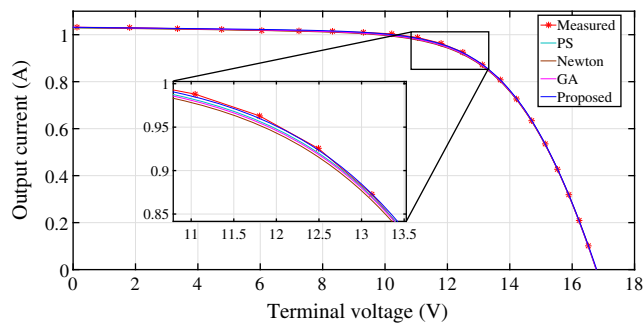
The errors where the measured current in the third column from left is compared with those predicted by the proposed method and other reference methods.

| Measured values | | | Absolute of current error (%) | | | | | | | | |
|---------------------|---------|---------|-------------------------------|-------|-------|-------|-------|-------|--------------|-------|--------|
| # | V (V) | I (A) | Proposed | LMSA | CPSO | SA | PS | BMO | ABSO | GA | Newton |
| 1 | 0.0057 | 0.7605 | 0.012 | 0.046 | 0.046 | 0.128 | 0.097 | 0.060 | 0.045 | 0.122 | 0.042 |
| 2 | 0.0646 | 0.7600 | 0.066 | 0.125 | 0.112 | 0.064 | 0.041 | 0.163 | 0.128 | 0.059 | 0.121 |
| 3 | 0.1185 | 0.7590 | 0.053 | 0.128 | 0.103 | 0.076 | 0.060 | 0.165 | 0.133 | 0.070 | 0.123 |
| 4 | 0.1678 | 0.7580 | 0.033 | 0.009 | 0.046 | 0.227 | 0.214 | 0.017 | 0.002 | 0.219 | 0.016 |
| 5 | 0.2132 | 0.7570 | 0.008 | 0.117 | 0.071 | 0.111 | 0.097 | 0.148 | 0.126 | 0.100 | 0.109 |
| 6 | 0.2545 | 0.7555 | 0.061 | 0.059 | 0.006 | 0.175 | 0.152 | 0.070 | 0.070 | 0.156 | 0.049 |
| 7 | 0.2924 | 0.7540 | 0.080 | 0.049 | 0.006 | 0.183 | 0.137 | 0.057 | 0.060 | 0.149 | 0.035 |
| 8 | 0.3269 | 0.7505 | 0.247 | 0.114 | 0.165 | 0.333 | 0.242 | 0.160 | 0.103 | 0.276 | 0.139 |
| 9 | 0.3585 | 0.7465 | 0.236 | 0.111 | 0.149 | 0.301 | 0.135 | 0.154 | 0.102 | 0.210 | 0.158 |
| 10 | 0.3873 | 0.7385 | 0.317 | 0.217 | 0.233 | 0.360 | 0.085 | 0.294 | 0.212 | 0.231 | 0.313 |
| 11 | 0.4137 | 0.7280 | 0.004 | 0.085 | 0.098 | 0.007 | 0.418 | 0.114 | 0.084 | 0.163 | 0.106 |
| 12 | 0.4373 | 0.7065 | 0.096 | 0.070 | 0.025 | 0.078 | 0.482 | 0.089 | 0.076 | 0.075 | 0.434 |
| 13 | 0.4590 | 0.6755 | 0.049 | 0.027 | 0.094 | 0.083 | 0.773 | 0.048 | 0.015 | 0.162 | 0.641 |
| 14 | 0.4784 | 0.6320 | 0.250 | 0.189 | 0.255 | 0.280 | 1.041 | 0.283 | 0.175 | 0.182 | 0.976 |
| 15 | 0.4960 | 0.5730 | 0.276 | 0.179 | 0.206 | 0.258 | 1.003 | 0.284 | 0.168 | 0.145 | 1.787 |
| 16 | 0.5119 | 0.4990 | 0.038 | 0.128 | 0.190 | 0.110 | 0.496 | 0.194 | 0.033 | 0.961 | 3.376 |
| 17 | 0.5265 | 0.4130 | 0.005 | 0.159 | 0.384 | 0.269 | 0.027 | 0.288 | 0.589 | 1.734 | 5.538 |
| 18 | 0.5398 | 0.3165 | 0.218 | 0.314 | 0.808 | 0.603 | 0.850 | 0.720 | 0.058 | 2.846 | 9.498 |
| 19 | 0.5521 | 0.2120 | 0.330 | 0.053 | 1.048 | 0.580 | 1.844 | 0.250 | 0.074 | 3.828 | 17.361 |
| 20 | 0.5633 | 0.1035 | 0.580 | 1.262 | 1.073 | 0.483 | 3.469 | 7.182 | 1.494 | 4.307 | 41.975 |
| MAE (%) | | | <u>0.148</u> | 0.172 | 0.256 | 0.236 | 0.583 | 0.537 | 0.187 | 0.800 | 4.140 |
| MAE of 4 points (%) | | | 0.100 | 0.093 | 0.118 | 0.112 | 0.678 | 0.134 | <u>0.088</u> | 0.145 | 0.539 |

Table 5

A panel parameters extracted by the proposed and other methods. The panel is composed of 36 cells ($C = 36$). The figures in parenthesis are the difference when the values obtained by the proposed methods are compared with those of other methods.

| | Proposed | PS | Newton | Ref. [14] | SA | MPCOA | GA |
|---------------------|------------------|--------------------|--------------------|---------------------|---------------------|---------------------|---------------------|
| Cn | 47.1816 (n/a) | 48.289 (+2.29%) | 48.45 (+2.62%) | 48.1862 (+2.08%) | 48.8211 (+3.36%) | 48.5065 (+2.73%) | 48.5862 (+2.98%) |
| CR_s (Ω) | 1.2744 (n/a) | 1.2053 (−5.73%) | 1.2057 (−5.70%) | 1.203 (−5.94%) | 1.1989 (−6.30%) | 1.20295 (−5.94%) | 1.1968 (−6.09%) |
| CR_p (Ω) | 715.824 (n/a) | 714.29 (−0.26%) | 555.56 (−28.9%) | 555.556 (−28.8%) | 833.333 (+14.1%) | 849.693 (+15.8%) | 555.556 (−22.4%) |
| I_S (μA) | 2.3326 (n/a) | 3.1756 (+26.6%) | 3.2875 (+29.0%) | 3.076 (+24.2%) | 3.6642 (+36.3%) | 3.3737 (+30.9%) | 3.436 (+47.3%) |
| I_{ph} (A) | 1.0333 (n/a) | 1.0313 (−0.19%) | 1.0318 (−0.15%) | 1.0339 (+0.06%) | 1.0331 (−0.02%) | 1.03188 (−0.14%) | 1.0441 (+1.05%) |

**Fig. 9.** The I – V curves of a panel modeled by the proposed and three other methods.

mathematical models built from calculated parameters are very close to the actual ones.

4.2. Extraction using standard datasets

In this part, the proposed technique is used to extract parameters from standard datasets of a solar cell, and of a PV panel. These

datasets have also been used, and extraction results were published in many papers. Our results are compared with theirs in order to check accuracy of our method.

4.2.1. Extraction on a reference cell

A dataset, which includes twenty measured I – V pairs, is shown in the second and third columns of Table 4. The measurements are carried out on a 57 mm-diameter commercial solar cell at temperature $T = 33^\circ C$ [12]. The dataset does not contain V_{OC} , I_{SC} , V_M nor I_M . These values are obtained by interpolation from the dataset as follows: $V_{OC} = 0.5727$ V, $I_{SC} = 0.7605$ A, $V_M = 0.45$ V and $I_M = 0.69$ A.

Table 3 shows the extracted parameters, calculated by the proposed method and by eight reference techniques: LMSA [25], CPSO [21], SA [23], PS [18], BMO [20], ABSO [22], GA [17], and Newton [12]. Note that all of them belong to the second group. In other words, they require lots of measurements and complex calculation. Although the proposed method employs only three I – V pairs, the extracted parameters are in the same range with those calculated by other techniques. Particularly, when compared with those obtained by LMSA, the discrepancy in n , R_s , and I_{ph} is -0.93% , -0.56% , and -0.03% respectively.

Table 6

The errors where the measured current in the third column from left is compared with those predicted by the proposed method and other reference methods.

| Measured values | | | Absolute of current error (%) | | | | | | |
|---------------------|---------|--------|-------------------------------|-------|--------|-----------|-------|-------|-------|
| # | V (V) | I (A) | Proposed | PS | Newton | Ref. [10] | SA | MPCOA | GA |
| 1 | 0.1248 | 1.0315 | 0.016 | 0.207 | 0.213 | 0.008 | 0.006 | 0.119 | 0.988 |
| 2 | 1.8093 | 1.0300 | 0.097 | 0.294 | 0.367 | 0.160 | 0.062 | 0.168 | 0.845 |
| 3 | 3.3511 | 1.0260 | 0.071 | 0.123 | 0.258 | 0.048 | 0.137 | 0.037 | 0.966 |
| 4 | 4.7622 | 1.0220 | 0.254 | 0.055 | 0.138 | 0.076 | 0.341 | 0.247 | 1.099 |
| 5 | 6.0538 | 1.0180 | 0.425 | 0.222 | 0.023 | 0.194 | 0.531 | 0.443 | 1.224 |
| 6 | 7.2364 | 1.0155 | 0.404 | 0.196 | 0.099 | 0.122 | 0.521 | 0.440 | 1.155 |
| 7 | 8.3189 | 1.0140 | 0.187 | 0.041 | 0.383 | 0.153 | 0.292 | 0.223 | 0.876 |
| 8 | 9.3097 | 1.0100 | 0.010 | 0.250 | 0.636 | 0.395 | 0.082 | 0.029 | 0.626 |
| 9 | 10.2163 | 1.0035 | 0.309 | 0.600 | 1.028 | 0.769 | 0.281 | 0.307 | 0.237 |
| 10 | 11.0449 | 0.9880 | 0.334 | 0.668 | 1.139 | 0.855 | 0.374 | 0.368 | 0.135 |
| 11 | 11.8018 | 0.9630 | 0.312 | 0.675 | 1.189 | 0.869 | 0.418 | 0.371 | 0.102 |
| 12 | 12.4929 | 0.9255 | 0.205 | 0.587 | 1.144 | 0.780 | 0.378 | 0.288 | 0.174 |
| 13 | 13.1231 | 0.8725 | 0.057 | 0.269 | 0.867 | 0.451 | 0.115 | 0.008 | 0.495 |
| 14 | 13.6983 | 0.8075 | 0.012 | 0.286 | 0.919 | 0.446 | 0.188 | 0.035 | 0.505 |
| 15 | 14.2221 | 0.7265 | 0.151 | 0.016 | 0.648 | 0.113 | 0.061 | 0.194 | 0.868 |
| 16 | 14.6995 | 0.6345 | 0.189 | 0.198 | 0.487 | 0.107 | 0.192 | 0.309 | 1.154 |
| 17 | 15.1346 | 0.5345 | 0.056 | 0.115 | 0.575 | 0.076 | 0.067 | 0.226 | 1.240 |
| 18 | 15.5311 | 0.4275 | 0.140 | 0.270 | 0.405 | 0.295 | 0.187 | 0.311 | 1.666 |
| 19 | 15.8929 | 0.3185 | 0.031 | 0.122 | 0.735 | 0.004 | 0.232 | 0.057 | 1.738 |
| 20 | 16.2229 | 0.2085 | 0.144 | 0.775 | 1.222 | 0.496 | 0.906 | 0.302 | 2.030 |
| 21 | 16.5241 | 0.1010 | 0.297 | 5.153 | 5.002 | 4.438 | 5.287 | 0.990 | 0.520 |
| MAE (%) | | | <u>0.176</u> | 0.530 | 0.832 | 0.517 | 0.508 | 0.261 | 0.888 |
| MAE of 4 points (%) | | | <u>0.147</u> | 0.454 | 1.030 | 0.636 | 0.275 | 0.175 | 0.319 |

Table 7

The input data, extracted parameters, the error of voltage, current at MPPs. The extractions are performed on four commercial panels by the method in [28], and by this method.

| | | GS601456P-218 | KC175GHT-2 | HIP-230 HDE1 | S75 |
|---------------------|------|---------------|------------|--------------|----------|
| C (No. of cells) | | 60 | 48 | 60 | 36 |
| V_{OC} (V) | | 36.30 | 29.35 | 42.46 | 21.55 |
| I_{SC} (A) | | 8.19 | 8.07 | 7.26 | 4.70 |
| V_M (V) | | 29.00 | 23.60 | 34.00 | 17.50 |
| I_M (A) | | 7.55 | 7.57 | 6.87 | 4.32 |
| n | [28] | 1.1841 | 0.9425 | 0.6078 | 1.0274 |
| | This | 1.435 | 1.1581 | 1.1253 | 1.4899 |
| R_s (m Ω) | [28] | 4.433 | 5.375 | 13.567 | 8.472 |
| | This | 3.427 | 4.858 | 8.215 | 3.033 |
| R_p (Ω) | [28] | 2.548 | 2.614 | 12.139 | 4.399 |
| | This | 13.965 | 90.241 | 587.2 | 14.612 |
| I_s (μ A) | [28] | 1.84E–08 | 8.46E–11 | 1.50E–19 | 6.46E–10 |
| | This | 6.04E–07 | 9.49E–09 | 1.68E–10 | 7.47E–07 |
| I_{ph} (A) | [28] | 8.1926 | 8.0698 | 7.2567 | 4.6948 |
| | This | 8.1920 | 8.0704 | 7.2601 | 4.7010 |
| V_M (V) | [28] | 29.2126 | 23.9257 | 33.5737 | 17.464 |
| | This | 29.0225 | 23.6155 | 34.0127 | 17.5133 |
| I_M (A) | [28] | 7.5 | 7.4768 | 6.9691 | 4.2381 |
| | This | 7.5481 | 7.5691 | 6.8712 | 4.3189 |
| Error of V_M (%) | [28] | –0.73% | –1.38% | 1.25% | 0.21% |
| | This | –0.08% | –0.07% | –0.04% | –0.08% |
| Error of I_M (%) | [28] | 0.66% | 1.23% | –1.44% | 1.90% |
| | This | 0.03% | 0.01% | –0.02% | 0.03% |

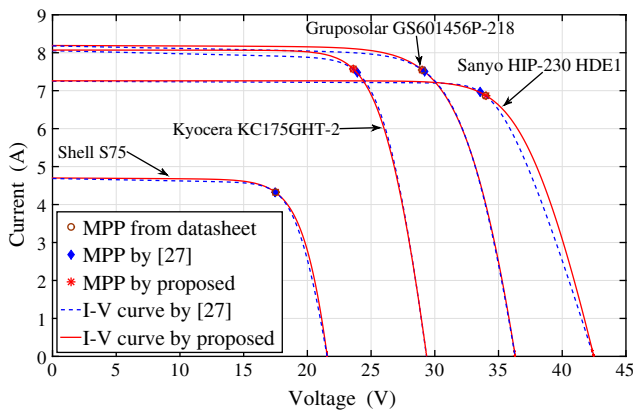


Fig. 10. The MPPs and I – V curves of four commercial panels modeled by the proposed method (red line) and by [28] (blue dash line). (For interpretation of the references to colour in this figure legend, the reader is referred to the web version of this article.)

Sets of calculated parameters are applied to the MATLAB – Simulink's solar cell model for simulation. The simulated I – V curves and the measured points are plotted in Fig. 8. The curve, modeled by our method are closed to all measured points, particularly around the MPP (zoomed part).

Table 4 also shows the discrepancy in current between experiment and calculation on all twenty points. Given V , the cell modeled by the proposed method estimates the current with 0.148% MAE. For this dataset, the results from the proposed method agree very much with the values by experiment, as reflected by the MAE of all points and that of the four points around the MPP. This means the proposed extracted method generates sets of parameters which are very reliable to compute the I – V pairs. This high accuracy depends on quality of the estimated I_M and V_M . For example, if the I – V pair at #13 (2.0% difference in V and –2.1% in I when compared to the interpolated point), which yields the highest product among the measured points is used as the MPP, the MAE would increase to 4.56%.

Table 8

Means of current error (%) when each of n , R_s , R_p , I_s and I_{ph} has percentage error as stated in the first column individually.

| Error by (%) | Mean of current error (%) | | | |
|--------------|---------------------------|-------|-------|-------|
| | n | R_s | R_p | I_s |
| –10 | 15.67 | –0.89 | 0.14 | –4.22 |
| –9 | 13.34 | –0.81 | 0.13 | –3.78 |
| –8 | 16.30 | –0.70 | 0.11 | –3.37 |
| –7 | 13.54 | –0.64 | 0.10 | –2.93 |
| –6 | 10.52 | –0.54 | 0.09 | –2.48 |
| –5 | 12.87 | –0.46 | 0.07 | –2.04 |
| –4 | 9.85 | –0.35 | 0.07 | –1.67 |
| –3 | 10.89 | –0.26 | 0.06 | –1.24 |
| –2 | 6.96 | –0.16 | 0.03 | –0.82 |
| –1 | 6.05 | –0.08 | 0.00 | –0.39 |
| 1 | –5.59 | 0.09 | –0.01 | 0.46 |
| 2 | –10.69 | 0.23 | –0.02 | 0.85 |
| 3 | –15.44 | 0.30 | –0.03 | 1.24 |
| 4 | –19.77 | 0.38 | –0.04 | 1.64 |
| 5 | –23.72 | 0.47 | –0.04 | 2.06 |
| 6 | –27.35 | 0.55 | –0.06 | 2.46 |
| 7 | –30.57 | 0.67 | –0.07 | 2.84 |
| 8 | –33.55 | 0.75 | –0.08 | 3.27 |
| 9 | –36.26 | 0.82 | –0.09 | 3.67 |
| 10 | –38.65 | 0.94 | –0.12 | 4.05 |

4.2.2. Extraction on a reference panel

Measurements are carried out on a panel, which is composed of 36 polycrystalline silicon cells in series at $T = 45^\circ\text{C}$ [12]. The experiment dataset is performed in Table 6 (left). Using interpolation, we get: $V_{OC} = 16.78$ V, $I_{SC} = 1.0315$ A, $V_M = 12.64$ V, and $I_M = 0.913$ A. For convenience in comparison, n , R_s , and R_p are multiplied by 36 (C).

Similar to Table 3, parameters extracted by the proposed approach are shown and compared with those obtained by six other methods in Table 5. These calculated sets are subsequently applied into the Simulink's solar cell model to obtain the I – V curves. Fig. 9 shows the I – V curves of four models (of the same panel) together with the measured points. The I – V curve of panel model by proposed methods is closed to the measured points, especially the points near the MPP (see the enlarged part). To

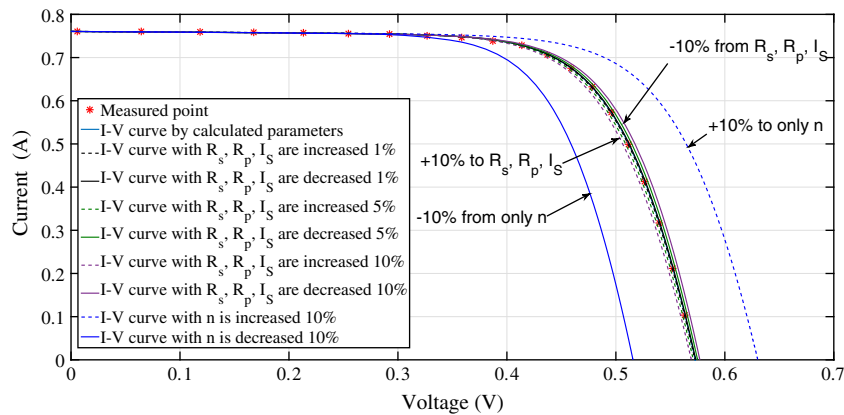


Fig. 11. The error in n has more effect on the I - V curves than those of R_s , R_p and I_s .

Table 9

The parameters of polycrystalline panels obtained by the proposed method using only the information in their datasheet (measured at the STC condition).

| Manufacturer, model | Given values in datasheet | | | | | Extracted parameters by proposed method | | | | |
|--------------------------|---------------------------|-----------|-----------|--------------|--------------|---|---------------------|--------------------|------------------|--------------|
| | C | V_m (V) | I_m (A) | V_{OC} (V) | I_{SC} (A) | n | R_s (m Ω) | R_p (Ω) | I_s (μ A) | I_{ph} (A) |
| WW Energy, AS240-6P30 | 60 | 29.90 | 8.03 | 37.70 | 8.57 | 1.1725 | 5.790 | 94.87 | 0.0074 | 8.5705 |
| WW Energy, AS245-6P30 | 60 | 30.10 | 8.14 | 37.90 | 8.66 | 1.1193 | 6.018 | 149.22 | 0.0025 | 8.6603 |
| H&T GmbH, TS240PB60 | 60 | 29.98 | 8.01 | 37.23 | 8.66 | 1.4373 | 2.946 | 15.89 | 0.4311 | 8.6616 |
| H&T GmbH, TS245PB60 | 60 | 30.11 | 8.14 | 37.34 | 8.82 | 1.4798 | 2.585 | 12.61 | 0.6773 | 8.8218 |
| H&T GmbH, TS285PB72 | 72 | 36.10 | 7.91 | 44.68 | 8.74 | 1.7058 | 1.124 | 3.61 | 6.0338 | 8.7427 |
| H&T GmbH, TS290PB72 | 72 | 36.18 | 8.02 | 44.81 | 8.85 | 1.7009 | 1.224 | 3.85 | 5.6358 | 8.8528 |
| H&T GmbH, TS285P72 | 72 | 35.60 | 8.00 | 44.51 | 8.52 | 1.1362 | 5.241 | 110.71 | 0.0054 | 8.5204 |
| H&T GmbH, TS290P72 | 72 | 35.86 | 8.09 | 44.65 | 8.64 | 1.2070 | 4.49 | 67.07 | 0.0177 | 8.6406 |
| Toenergy, TN-P230 | 60 | 29.50 | 8.42 | 36.60 | 7.80 | 1.3902 | 3.046 | 18.25 | 0.3184 | 8.4214 |
| Toenergy, TN-P235 | 60 | 30.00 | 8.46 | 27.20 | 7.83 | 1.4292 | 2.945 | 16.80 | 0.3881 | 8.4615 |
| Kyocera, KD330GX-LFB | 80 | 40.50 | 8.15 | 49.90 | 8.79 | 1.4230 | 2.477 | 17.16 | 0.3382 | 8.7913 |
| Kyocera, KU325-8BCA | 80 | 40.40 | 8.05 | 50.00 | 8.68 | 1.4111 | 2.926 | 19.37 | 0.2795 | 8.6813 |
| Kyocera, KD145 SX-UFU | 36 | 17.90 | 8.11 | 22.30 | 8.78 | 1.4491 | 3.048 | 14.64 | 0.5154 | 8.7818 |
| Kyocera, KD100-36 | 36 | 17.70 | 7.91 | 22.10 | 8.68 | 1.6199 | 2.169 | 5.86 | 3.3444 | 8.6832 |
| Green Stealth, GS-PV4175 | 72 | 35.40 | 4.90 | 44.50 | 5.50 | 1.8456 | 2.306 | 3.800 | 11.59 | 5.5033 |
| Nemy, JB250P60 | 60 | 30.10 | 8.31 | 37.50 | 8.85 | 1.1585 | 4.799 | 101.16 | 0.0066 | 8.8504 |
| Nemy, JB255P60 | 60 | 30.50 | 8.39 | 37.80 | 8.95 | 1.2163 | 4.140 | 71.11 | 0.0155 | 8.9505 |
| Nemy, JB300P72 | 72 | 36.50 | 8.12 | 45.30 | 8.79 | 1.4793 | 2.775 | 14.06 | 0.5610 | 8.7917 |
| Nemy, JB305P72 | 72 | 37.40 | 8.16 | 45.60 | 9.05 | 1.6872 | 0.254 | 2.30 | 3.9351 | 9.0510 |
| Scheuten, Gold-P6-54 | 54 | 27.40 | 7.85 | 33.50 | 8.30 | 1.0523 | 4.343 | 261.88 | 0.0009 | 8.3001 |
| Scheuten, Gold-P6-54 | 54 | 27.60 | 7.97 | 33.60 | 8.44 | 1.0997 | 3.687 | 173.31 | 0.0023 | 8.4402 |
| Scheuten, i40P6-60 | 60 | 29.90 | 8.03 | 37.00 | 8.58 | 1.2268 | 3.899 | 55.82 | 0.0270 | 8.5806 |
| Scheuten, i40P6-60 | 60 | 30.10 | 8.13 | 37.10 | 8.69 | 1.2482 | 3.472 | 48.87 | 0.0364 | 8.6906 |
| Scheuten, Mult-P6-66 | 66 | 33.80 | 7.99 | 41.10 | 8.46 | 1.1007 | 3.597 | 173.15 | 0.0023 | 8.4602 |
| Scheuten, Mult-P6-66 | 66 | 34.00 | 8.09 | 41.30 | 8.57 | 1.1191 | 3.410 | 153.59 | 0.0030 | 8.5702 |
| Sharp, NDR235A5 | 60 | 30.30 | 7.76 | 36.80 | 8.49 | 1.5600 | 0.459 | 4.22 | 1.8720 | 8.4909 |
| Sharp, NDR240A5 | 60 | 30.40 | 7.90 | 37.20 | 8.57 | 1.5108 | 1.444 | 9.13 | 0.9756 | 8.5714 |
| Fabrik, Pro. 54 | 54 | 27.21 | 8.46 | 33.95 | 9.02 | 1.1841 | 4.730 | 86.48 | 0.0094 | 9.0205 |
| Fabrik, Pro. 54 | 54 | 27.47 | 8.56 | 34.23 | 9.11 | 1.1604 | 4.825 | 111.72 | 0.0053 | 9.1104 |
| Solarworld, SW50RMA | 36 | 18.20 | 2.75 | 22.10 | 2.95 | 1.3412 | 5.236 | 65.65 | 0.0534 | 2.9502 |
| Solarworld, SW80RNA | 36 | 17.90 | 4.49 | 21.90 | 4.78 | 1.1696 | 5.921 | 134.63 | 0.0076 | 4.7802 |
| Solarworld, SW130R6A | 36 | 17.40 | 7.49 | 21.50 | 7.99 | 1.1613 | 4.121 | 71.22 | 0.0160 | 7.9905 |
| Solarworld, SW140R6A | 36 | 18.00 | 7.85 | 22.10 | 8.35 | 1.1539 | 3.844 | 95.56 | 0.0084 | 8.3503 |
| Solarworld, Pro. SW250 | 60 | 30.50 | 8.27 | 37.60 | 8.81 | 1.1974 | 3.887 | 79.43 | 0.0124 | 8.8104 |
| Solarworld, Pro. SW255 | 60 | 30.90 | 8.32 | 38.00 | 8.88 | 1.2554 | 3.457 | 57.40 | 0.0261 | 8.8805 |

evaluate the accuracy of the proposed method and the other referenced techniques, the differences of current at 21 measured points are calculated and shown in Table 6. MAE of the panel model by proposed method is only 0.176%.

On both standard datasets, our MAEs are smaller than those of the others' models. This confirms that our method yields high accuracy, but it requires only the measurement on the OSMP, and for the panel temperature.

4.3. Calculations using OSMP from product datasheets

To gain acceptance in usefulness, four PV panels, whose parameters were extracted by [28], will be extracted again by our technique in this part. Those panels include Gruposolar GS601456P-218, Kyocera KC175GHT-2, Sanyo HIP-230 HDE1, and Shell S75.

Table 7 shows the required data from the datasheets (in the top rows), extracted parameters (in the middle row), and error in

voltage and in current at MPP (in the bottom rows). Extracted parameters by both methods are applied into the MATLAB – Simulink's solar panel model to simulate and plot the I – V curves (Fig. 10). The MPP predicted by both methods are compared. For all four panels, with the same inputs, MPPs calculated by our technique are closer to the actual MPPs than those calculated by [28].

To check validity of our technique, Tables 9–11 in Appendix A are presented with the extracted parameters of polycrystalline, of monocrystalline, and of thin-film panels respectively. All extractions use the information at the STC conditions in the product datasheets only. More than 180 PV panels were extracted by our proposed method. The results are available at [26].

4.4. Effects of parameter errors on I – V curve

The extracted parameters of the cell in Section 4.2.1 are used to analyze the effect of each parameter's error to the I – V curve. Almost all techniques approximate I_{ph} very close to I_{sc} . So its error is not considered. Each of other four parameters is added by relative error of -10% to $+10\%$ with a step of 1% . With every new value of each parameter, a model of solar cell is created. Next, the means of differences between calculated current using the model with a parameter's error and the measured current, at twenty given voltages are calculated. The results are shown in Table 8. The second column shows that error in n leads to rapid error in the calculated current. According to the data in the next three columns, the errors in R_s , R_p and I_s have less effect on the current. This can be easily seen in their effects to the I – V curves in Fig. 11. The curve is

shifted not much even if R_s , R_p and I_s are all changed by $+10\%$. On the other hand, if n is changed by 10% (or -10%), the I – V curve move towards the right (or left) by a relatively long distance.

5. Conclusion

The experiments and calculations confirm that our proposed technique can extract parameters for the single-diode model of solar cells. Furthermore, they show that our results are even more accurate than those of the techniques, which require complex calculation and lots of measurements. It requires only good measurement of the panel temperature and the OSMP (T , V_{oc} , I_{sc} , V_m and I_m). PV panel manufacturers always provide these parameters when operating at the STC conditions in their datasheets. Extractions using information from the experiments, and from the standard datasets yield parameters, whose I – V relation matches the measured pairs nicely. Parameters of several panels are then extracted using only the information in their datasheets. All the outcomes are within valid ranges.

It is noteworthy that this technique is not suitable for the PV panels that are made from multi-junction solar cells.

Manufacturers sometimes provide information on the effect of temperature and irradiance in their datasheets. In this case, measurements are not required. Parameters at any operating conditions may be estimated from ones obtained at the STC conditions. However, if ones need accurate parameters, or to update the aging effect of the panels, measurements are still needed.

Table 10

The parameters of monocrystalline panels obtained by the proposed method using only the information in their datasheet (measured at the STC condition).

| Manufacturer, model | Given values in datasheet | | | | | Extracted parameters by proposed method | | | | |
|------------------------|---------------------------|-----------|-----------|--------------|--------------|---|---------------------|--------------------|------------------|--------------|
| | C | V_m (V) | I_m (A) | V_{oc} (V) | I_{sc} (A) | n | R_s (m Ω) | R_p (Ω) | I_s (μ A) | I_{ph} (A) |
| Solarworld, Plus SW260 | 60 | 30.70 | 8.56 | 38.90 | 9.18 | 1.2918 | 5.464 | 51.70 | 0.0298 | 9.1810 |
| Solarworld, Plus SW270 | 60 | 30.90 | 8.81 | 39.20 | 9.44 | 1.2809 | 5.546 | 57.51 | 0.0223 | 9.4409 |
| Solarworld, Plus SW280 | 60 | 31.20 | 9.07 | 39.50 | 9.71 | 1.2793 | 5.357 | 61.07 | 0.0192 | 9.7109 |
| Nemy, JP260M60 | 60 | 30.70 | 8.47 | 38.10 | 9.14 | 1.4403 | 2.980 | 18.20 | 0.3186 | 9.1415 |
| Nemy, JP265M60 | 60 | 31.00 | 8.56 | 38.30 | 9.16 | 1.3043 | 3.476 | 43.05 | 0.0483 | 9.1607 |
| Nemy, JP270M60 | 60 | 31.10 | 8.68 | 38.60 | 9.20 | 1.1027 | 5.013 | 207.73 | 0.0013 | 9.2002 |
| AXSun, AXM280-60 | 60 | 31.49 | 8.89 | 38.74 | 9.50 | 1.3037 | 3.188 | 46.39 | 0.0399 | 9.5007 |
| AXSun, AXM285-60 | 60 | 31.75 | 8.98 | 39.06 | 9.59 | 1.3013 | 3.256 | 50.66 | 0.0332 | 9.5906 |
| AXSun, AXM290-60 | 60 | 32.01 | 9.06 | 39.38 | 9.68 | 1.3217 | 3.200 | 47.42 | 0.0386 | 9.6807 |
| H&T GmbH, TS185D72 | 72 | 36.42 | 5.08 | 45.05 | 5.41 | 1.1796 | 6.858 | 144.16 | 0.0058 | 5.4103 |
| H&T GmbH, TS195D72 | 72 | 36.94 | 5.28 | 45.28 | 5.58 | 1.0497 | 6.997 | 454.87 | 0.0004 | 5.5801 |
| H&T GmbH, TS205D72 | 72 | 37.83 | 5.42 | 45.68 | 5.90 | 1.5558 | 0.551 | 7.41 | 0.7378 | 5.9004 |
| H&T GmbH, TS245D60 | 60 | 30.49 | 8.04 | 37.51 | 8.64 | 1.3674 | 2.764 | 24.77 | 0.1597 | 8.6410 |
| H&T GmbH, TS255D60 | 60 | 30.69 | 8.31 | 37.73 | 8.93 | 1.3769 | 2.633 | 23.86 | 0.1682 | 8.9310 |
| H&T GmbH, TS265D60 | 60 | 30.90 | 8.58 | 38.10 | 9.19 | 1.3213 | 3.174 | 36.45 | 0.0684 | 9.1908 |
| H&T GmbH, TS295D72 | 72 | 36.48 | 8.09 | 45.01 | 8.71 | 1.3931 | 2.801 | 21.28 | 0.2236 | 8.7111 |
| H&T GmbH, TS305D72 | 72 | 36.72 | 8.31 | 45.28 | 8.92 | 1.3488 | 3.013 | 28.71 | 0.1159 | 8.9209 |
| H&T GmbH, TS315D72 | 72 | 36.91 | 8.53 | 45.62 | 9.12 | 1.2765 | 3.596 | 48.51 | 0.0367 | 9.1207 |
| Fabrik, Premium255L | 60 | 30.45 | 8.40 | 37.80 | 8.90 | 1.0718 | 5.136 | 225.46 | 0.0010 | 8.9002 |
| Fabrik, Premium265L | 60 | 30.85 | 8.60 | 38.10 | 9.20 | 1.2926 | 3.444 | 44.06 | 0.0452 | 9.2007 |
| Fabrik, Premium275L | 60 | 31.25 | 8.80 | 38.50 | 9.50 | 1.4800 | 2.266 | 14.91 | 0.4400 | 9.5014 |
| Fabrik, Premium200XM | 48 | 24.25 | 8.25 | 30.09 | 8.73 | 1.0414 | 5.334 | 292.56 | 0.0006 | 8.7302 |
| Fabrik, Premium205XM | 48 | 24.56 | 8.35 | 30.40 | 8.83 | 1.0448 | 5.204 | 316.96 | 0.0005 | 8.8301 |
| Fabrik, Premium210XM | 48 | 24.86 | 8.45 | 30.70 | 8.93 | 1.0475 | 5.083 | 339.33 | 0.0004 | 8.9301 |
| Sky Energy, STM300 | 72 | 37.00 | 8.13 | 45.20 | 8.74 | 1.3960 | 2.099 | 20.40 | 0.2162 | 8.7409 |
| Sky Energy, STM305 | 72 | 37.20 | 8.22 | 45.50 | 8.76 | 1.2370 | 3.203 | 64.58 | 0.0201 | 8.7604 |
| Sky Energy, STM310 | 72 | 37.60 | 8.27 | 45.60 | 8.80 | 1.2317 | 2.637 | 67.24 | 0.0177 | 8.8003 |
| Soluxtec, Dark T245 | 60 | 29.80 | 8.25 | 37.42 | 8.80 | 1.1650 | 5.307 | 92.43 | 0.0078 | 8.8005 |
| Soluxtec, Dark T250 | 60 | 30.15 | 8.30 | 37.55 | 8.85 | 1.1852 | 4.635 | 83.71 | 0.0104 | 8.8505 |
| Sunpower, E19/240 | 72 | 40.50 | 5.93 | 48.60 | 6.30 | 1.3064 | 2.852 | 98.36 | 0.0115 | 6.3002 |
| Sunpower, E19/320 | 96 | 54.70 | 5.86 | 64.80 | 6.24 | 1.3766 | 0.860 | 40.48 | 0.0317 | 6.2401 |
| Sunpower, E19/425 | 128 | 72.90 | 5.83 | 85.60 | 6.21 | 1.3370 | 0.116 | 19.03 | 0.0215 | 6.2100 |

Table 11

The parameters of tin film panels obtained by the proposed method using only the information in their datasheet (measured at the STC condition).

| Manufacturer, model | Given values in datasheet | | | | | Extracted parameters by proposed method | | | | |
|-----------------------|---------------------------|-----------|-----------|--------------|--------------|---|---------------------|--------------------|------------------|--------------|
| | C | V_m (V) | I_m (A) | V_{OC} (V) | I_{SC} (A) | n | R_s (m Ω) | R_p (Ω) | I_s (μ A) | I_{ph} (A) |
| FirstSolar, FS-375 | 154 | 46.90 | 1.60 | 60.10 | 1.82 | 1.2425 | 6.826 | 5.88 | 8.5610 | 1.8221 |
| FirstSolar, FS-377 | 154 | 48.30 | 1.61 | 60.70 | 1.84 | 1.2387 | 2.508 | 4.35 | 7.2738 | 1.8411 |
| FirstSolar, FS-380 | 154 | 48.50 | 1.65 | 60.80 | 1.88 | 1.2248 | 2.320 | 4.48 | 6.3399 | 1.8810 |
| FirstSolar, FS-382 | 154 | 48.30 | 1.71 | 60.80 | 1.94 | 1.2240 | 3.269 | 5.07 | 6.5356 | 1.9413 |
| FirstSolar, FS-385 | 154 | 48.50 | 1.76 | 61.00 | 1.98 | 1.1937 | 3.940 | 6.32 | 4.6892 | 1.9812 |
| FirstSolar, FS-492A | 216 | 67.00 | 1.38 | 86.00 | 1.54 | 1.1515 | 12.287 | 13.37 | 2.1472 | 1.5414 |
| FirstSolar, FS-495A | 216 | 67.90 | 1.40 | 86.50 | 1.55 | 1.1073 | 11.770 | 17.37 | 1.1689 | 1.5511 |
| FirstSolar, FS-497A | 216 | 68.70 | 1.42 | 87.20 | 1.56 | 1.0760 | 11.436 | 24.17 | 0.7239 | 1.5500 |
| FirstSolar, FS-4100A | 216 | 69.40 | 1.44 | 87.60 | 1.57 | 1.0238 | 12.238 | 31.44 | 0.3121 | 1.5746 |
| FirstSolar, FS-4102-2 | 216 | 67.00 | 1.53 | 85.30 | 1.74 | 1.2518 | 5.736 | 5.91 | 7.7399 | 1.7417 |
| FirstSolar, FS-4105-2 | 216 | 67.80 | 1.55 | 86.00 | 1.74 | 1.1951 | 6.771 | 8.49 | 3.9337 | 1.7414 |
| FirstSolar, FS-4107-2 | 216 | 68.60 | 1.57 | 86.60 | 1.75 | 1.1616 | 6.774 | 10.45 | 2.4919 | 1.7511 |
| FirstSolar, FS-4110-2 | 216 | 69.40 | 1.59 | 87.20 | 1.75 | 1.0838 | 8.074 | 17.67 | 0.8670 | 1.7508 |
| FirstSolar, FS-4112-2 | 216 | 70.20 | 1.60 | 87.70 | 1.75 | 1.0439 | 8.027 | 23.57 | 0.4582 | 1.7506 |
| ISET(US), IXP66 | 108 | 44.00 | 1.50 | 54.00 | 2.00 | 1.2674 | 0.007 | 0.99 | 0.3178 | 2.0000 |
| ISET(US), IXP73 | 108 | 44.40 | 1.64 | 55.00 | 2.08 | 1.4406 | 0.040 | 1.28 | 1.7675 | 2.0801 |
| ISET(US), IXP80 | 108 | 44.80 | 1.79 | 56.00 | 2.15 | 1.6200 | 0.387 | 2.07 | 7.3396 | 2.1504 |
| Calyxo, CX375 | 154 | 46.30 | 1.65 | 62.00 | 1.95 | 1.4744 | 12.169 | 3.35 | 44.2710 | 1.9571 |
| Calyxo, CX377 | 154 | 46.70 | 1.68 | 62.50 | 1.98 | 1.4722 | 12.269 | 3.47 | 40.7130 | 1.9870 |
| Calyxo, CX380 | 154 | 47.00 | 1.72 | 62.80 | 2.01 | 1.4340 | 12.780 | 3.99 | 29.6930 | 2.0165 |
| Calyxo, CX382 | 154 | 47.30 | 1.75 | 63.20 | 2.04 | 1.4289 | 12.978 | 4.15 | 27.0550 | 2.0464 |
| Calyxo, CX385 | 154 | 47.80 | 1.78 | 63.60 | 2.06 | 1.3989 | 12.828 | 4.70 | 20.1080 | 2.0656 |
| XSUNX, XSC-150 | 96 | 42.60 | 3.52 | 54.90 | 3.91 | 1.5972 | 8.240 | 9.54 | 3.3926 | 3.9134 |
| XSUNX, XSC-170 | 96 | 44.60 | 3.81 | 56.20 | 4.19 | 1.5583 | 5.462 | 11.594 | 1.8354 | 4.1920 |
| XSUNX, XSC-185 | 96 | 46.50 | 3.98 | 57.60 | 4.38 | 1.6159 | 2.685 | 8.604 | 2.2649 | 4.3814 |
| Sunshine, SS1114120K | 162 | 57.69 | 2.13 | 85.25 | 2.62 | 1.9936 | 34.060 | 2.72 | 84.488 | 2.6532 |
| Sunshine, SS1114130K | 162 | 59.87 | 2.17 | 87.33 | 2.62 | 1.9372 | 33.001 | 3.47 | 48.9740 | 2.6452 |
| Sunshine, SS1114140K | 162 | 64.00 | 2.20 | 90.63 | 2.59 | 1.8918 | 28.874 | 4.95 | 24.8520 | 2.6052 |
| Sunshine, SS1114150K | 162 | 66.40 | 2.25 | 92.07 | 2.59 | 1.7747 | 26.352 | 7.47 | 9.6830 | 2.5992 |
| Sunshine, SS1114160K | 162 | 71.40 | 2.28 | 95.40 | 2.61 | 1.8866 | 17.277 | 7.05 | 13.3250 | 2.6164 |

Acknowledgment

The authors would like to thank the CU-ASEAN Scholarship and Department of Electrical Engineering, Chulalongkorn University, Bangkok, Thailand for their scholarship. Moreover, additional financial support by the Centre of Excellence in Electrical Power Technology, Chulalongkorn University, provides the facilities required by the research, which yields this paper.

Appendix A

Table 9 shows the input data and extracted parameters at STC of 35 polycrystalline panels using their datasheets.

Table 10 shows the input data and extracted parameters of 32 commercial monocrystalline solar panels.

Table 11 presents the input data and calculated parameters of 30 thin film solar panels.

The smallest and the highest of each parameters are underlined. All extracted parameters from datasheets are in the valid ranges.

References

- [1] Carrero C, Amador J, Arnaltes S. A single procedure for helping PV designers to select silicon PV modules and evaluate the loss resistances. *Renew Energy* 2007;32:2579–89.
- [2] Chin VJ, Salam Z, Ishaque K. Cell modelling and model parameters estimation techniques for photovoltaic simulator application: a review. *Appl Energy* 2015;154:500–19.
- [3] Cotfas DT, Cotfas PA, Kaplanis S. Methods to determine the dc parameters of solar cells: a critical review. *Renew Sustain Energy Rev* 2013;28:588–96.
- [4] Humada AM, Hojabri M, Mekhilef S, Hamada HM. Solar cell parameters extraction based on single and double-diode models: a review. *Renew Sustain Energy Rev* 2016;56:494–509.
- [5] Chan D, Phillips J, Phang J. A comparative study of extraction methods for solar cell model parameters. *Solid-State Electron* 1986;29:329–37.
- [6] Ishibashi K, Kimura Y, Niwano M. An extensively valid and stable method for derivation of all parameters of a solar cell from a single current–voltage characteristic. *J Appl Phys* 2008;103.
- [7] Tivanov M, Patryn A, Drozdov N, Fedotov A, Mazanik A. Determination of solar cell parameters from its current-voltage and spectral characteristics. *Sol Energy Mater Sol Cells* 2005;87:457–65.
- [8] Chegaar M, Azzouzi G, Mialhe P. Simple parameter extraction method for illuminated solar cells. *Solid-State Electron* 2006;50:1234–7.
- [9] El-Adawi MK, Al-Nuaim IA. A method to determine the solar cell series resistance from a single IV. Characteristic curve considering its shunt resistance new approach. *Vacuum* 2002;64:33–6.
- [10] Toledo FJ, Blanes JM. Analytical and quasi-explicit four arbitrary point method for extraction of solar cell single-diode model parameters. *Renew Energy* 2016;92:346–56.
- [11] Chen Y, Wang X, Li D, Hong R, Shen H. Parameters extraction from commercial solar cells IV characteristics and shunt analysis. *Appl Energy* 2011;88:2239–44.
- [12] Easwarakhanthan T, Bottin J, Bouhouch I, Boutrit C. Nonlinear minimization algorithm for determining the solar cell parameters with microcomputers. *Int J Sol Energy* 1986;4:1–12.
- [13] Conde AO, Sanchez FJG, Muci J. New method to extract the model parameters of solar cells from the explicit analytic solutions of their illuminated IV characteristics. *Sol Energy Mater Sol Cells* 2006;90:352–61.
- [14] Bouzidi K, Chegaar M, Nehaoua N. New method to extract the parameters of solar cells from their illuminated I–V curve. In: 4th International conference on computer integrated manufacturing. Setif, Algeria; November 2007.
- [15] Jiang LL, Maskell DL, Patra JC. Parameter estimation of solar cells and modules using an improved adaptive differential evolution algorithm. *Appl Energy* 2013;112:185–93.
- [16] Ishaque K, Salam Z, Mekhilef S, Shamsudin A. Parameter extraction of solar photovoltaic modules using penalty-based differential evolution. *Appl Energy* 2012;99:297–308.
- [17] AlRashidi MR, AlHajri MF, El-Naggar KM, Al-Othman KA. A new estimation approach for determining the IV characteristics of solar cells. *Sol Energy* 2011;85:1543–50.
- [18] Al-Hajri MF, El-Naggar KM, Al-Rashidi MR, Al-Othman AK. Optimal extraction of solar cell parameters using pattern search. *Renew Energy* 2012;44:238–45.
- [19] Patel SJ, Panchal AK, Kheraj V. Extraction of solar cell parameters from a single current–voltage characteristic using teaching learning based optimization algorithm. *Appl Energy* 2014;119:384–93.
- [20] Askarzadeh A, Rezaeadeh A. Extraction of maximum power point in solar cells using bird mating optimizer-based parameters identification approach. *Sol Energy* 2013;90:123–33.

- [21] Wei H, Cong J, Lingyun X, Deyun S. Extracting solar cell model parameters based on chaos particle swarm algorithm. In: International conference on electric information and control engineering (ICEICE). p. 398–402.
- [22] Askarzadeh A, Rezazadeh A. Artificial bee swarm optimization algorithm for parameters identification of solar cell models. *Appl Energy* 2013;102:943–9.
- [23] El-Naggar KM, AlRashidi MR, AlHajri MF, Al-Othman AK. Simulated annealing algorithm for photovoltaic parameters identification. *Sol Energy* 2012;86:266–74.
- [24] Xiaofang Y, Yongzhong X, Yuqing H. Parameter extraction of solar cell models using mutative-scale parallel chaos optimization algorithm. *Sol Energy* 2014;108:238–51.
- [25] Dkhichi F, Oukarfi B, Fakkar A, Belbounaguia N. Parameter identification of solar cell model using Levenberg–Marquardt algorithm combined with simulated annealing. *Sol Energy* 2014;110:781–8.
- [26] http://www.esid.ee.eng.chula.ac.th/index_research.htm.
- [27] Willsch B, Kumar P, Aabdin Z, Peranio N, Eibl O. Series and contact resistance measurements between 80 K and room temperature for industrial solar cells. *Energy Proc* 2015;67:49–63.
- [28] Orioli A, Gangi AD. A procedure to calculate the five-parameter model of crystalline silicon photovoltaic modules on the basis of the tabular performance data. *Appl Energy* 2013;102:1160–77.